Pictorial essay:

LLAMA SKULL VERSUS J-TYPE REPTILIAN TRIDACTYL SKULL: THE TRUTH?

An evidence-based comparison using CT scans with advanced 3D image reconstruction.

*By **Dr. K .H. Fung** (Hong Kong SAR, China)*

July 2026

ACKNOWLEDGEMENT

- The author wished to thank *Tridactyls.org (https://tridactyls.org)* for granting permission for use of the DICOM CT datasets available on their website for this scientific study.
- The author wished to thank *DigiMorph.org (https://www.digimorph.org)* for granting permission for use of the 3D CT model of *Lama glama* available on their website for this scientific study.

SECTION I: BACKGROUND

- A collection of desiccated corpses with 3 fingers and 3 toes collectively known as 'tridactyls' had been uncovered near the Palpa-Nazca region of Peru since 2016.
- The J-type tridactyls were referred to as 'reptilians' because they showed reptile-like skin and some could be found bearing eggs. They were about 60 cm in height, bipedal tridactyls showing distinct anatomy quite different from human or other known animals.
- A peer review paper by *José de la Cruz Ríos López et al* published in *International Journal of Biology & Biomedicine* in 2021 entitled '*Applying CT-scanning for the identification of a skull of an unknown archaeological find in Peru*' *(Reference 1)* had attempted to match a digitally dissected 3D model of llama cranium reversed back-for-front to the J-type tridactyl skull (without fully addressing the whole specimen). In his conclusion in page 63, he stated *(quote)* '***The "archaeological" find with an unknown form of "animal"*** (he was referring to tridactyl nicknamed '***Josephina***' aka '***Josefina***') ***was identified to have a head composed of a llama deteriorated braincase.***' This had sparked major controversies and hot debate over whether the whole discovery was a hoax in the subsequent years to follow.
- In order to dispel any worldwide misconception and controversies, there is a need to answer specifically the research question: "**Can a reversed dissected llama cranium mimic the skull of a J-type reptilian tridactyl?**"

SECTION II: MATERIALS & METHOD

- Llama skull: 3D CT model in (*.stl*) format of the skull of *Lama glama* (scientific name for llama) was downloaded from DigiMorph. *(Reference 2)* The whole llama skull was then digitally dissected to preserve the cranium, which was then reversed back-for-front as a "**reversed dissected llama cranium**" (RDLC) to match the tridactyl skulls for comparison.
- J-type tridactyl skull: DICOM CT datasets of J-type tridactyls nicknamed '***Josefina***', '***Luisa***' and '***Alberto***' were downloaded from Tridactyls.org. *(Reference 3)* 3D models were created using shaded-surface-display (SSD) by setting appropriate threshold for bone in DICOM software *Osirix* *(Reference 4)* and exported as (*.stl*) files. Digital segmentation was then performed to isolate the skull models using '*Meshmixer*' 3D modelling software. *(Reference 5)*
- CT scans inherently produce accurate sized 3D models useful for comparison. A vertical comparison (stacked) instead of side-by-side comparison to reduce parallax error of the models was then made in various standard projections. Similarly cut sections were also compared.
- Points of discrepancy were identified and labelled. Reference for anatomical labelling of *Lama glama* will be based largely on a paper by *Rosu et al* (2024). *(Reference 6)*

SECTION III: FINDINGS

Llama skull:

- The 3D model obtained from DigiMorph is a complete skull of *Lama glama*. *(Figure 1)*
- *López* made comparison based on CT imaging with 3D reconstruction using only the cranial segment of the llama skull and reversed it back-for-front in order to compare with the whole skull of the tridactyls.
- The cranium only occupies less than half of the posterior and superior portion of the llama skull.*(Figure 2)*
- If the tridactyl skull is constructed from a llama skull in a physical sense, a large part of the llama skull would have to be removed leaving very large cropped surfaces with inevitable machine marks easily identifiable on CT. *(Figure 3)*
- Since the large foramen magnum at the back of the llama skull is rotated forward to match the position of the mouth of the tridactyl skull, he also proposed to add in other animal bones fashioned as the tridactyl mouth apparatus in order to fill the hole. *López* did not specify what animal and how this could have been done precisely on an ancient skeleton nor did he showed any evidence. *(Figure 4)*

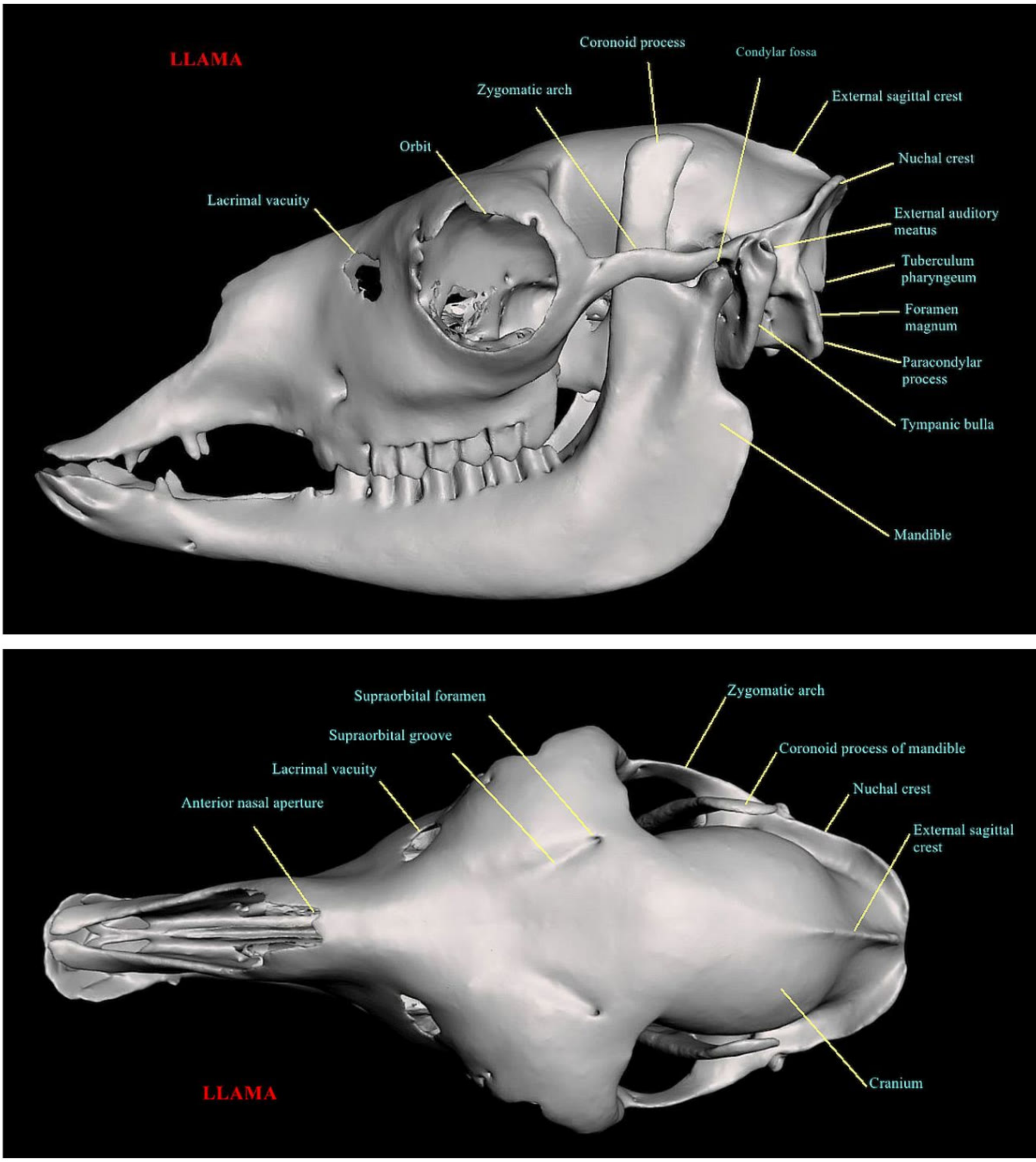

Figure 1: 3D CT model. Side view *(upper image)* and top view *(lower image)* of 3D digital model of llama skull (*Lama glama*) created from CT downloaded from DigiMorph showing labelled anatomy.

Figure 2: 3D CT model. Side view *(upper image)* and top view *(lower image)* of the 3D digital model of llama skull (*Lama glama*) in semi-transparency showing the location and relative size of the cranium *(in red)*.

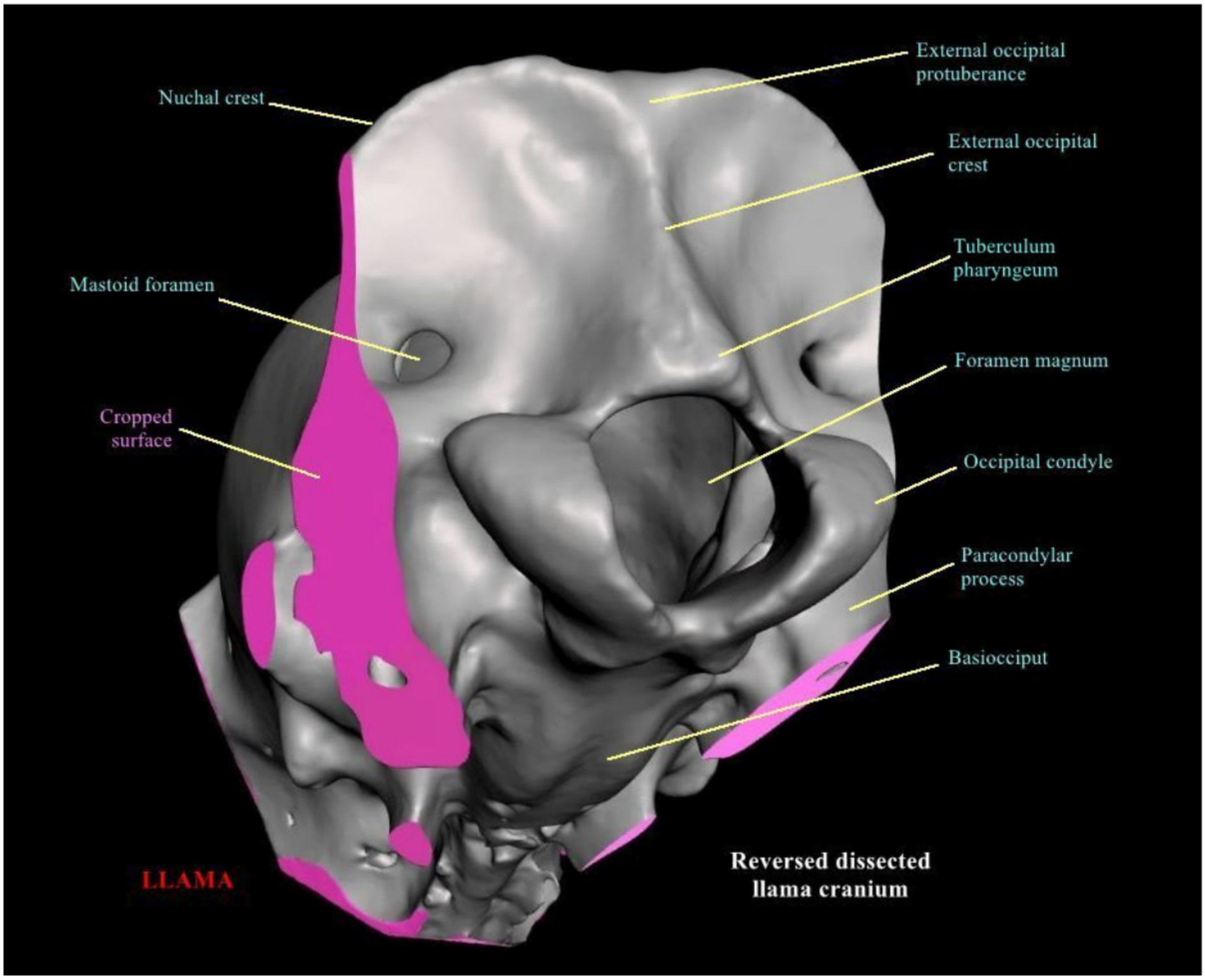

Figure 3: 3D CT model of the digitally dissected cranium of the llama skull viewed from the back. Note the extensive cut surfaces *(in pink)* needed in order to match the tridactyl skull. Such crop marks could not have escaped detection on 2D CT scans or 3D CT reconstruction. In the model used by *López*, the back of the cranium will be matching the face of the tridactyl by turning the llama cranium back-for-front. Note the big hole representing the foramen magnum that needed to be filled up in order to match the mouth apparatus of the tridactyl skull.

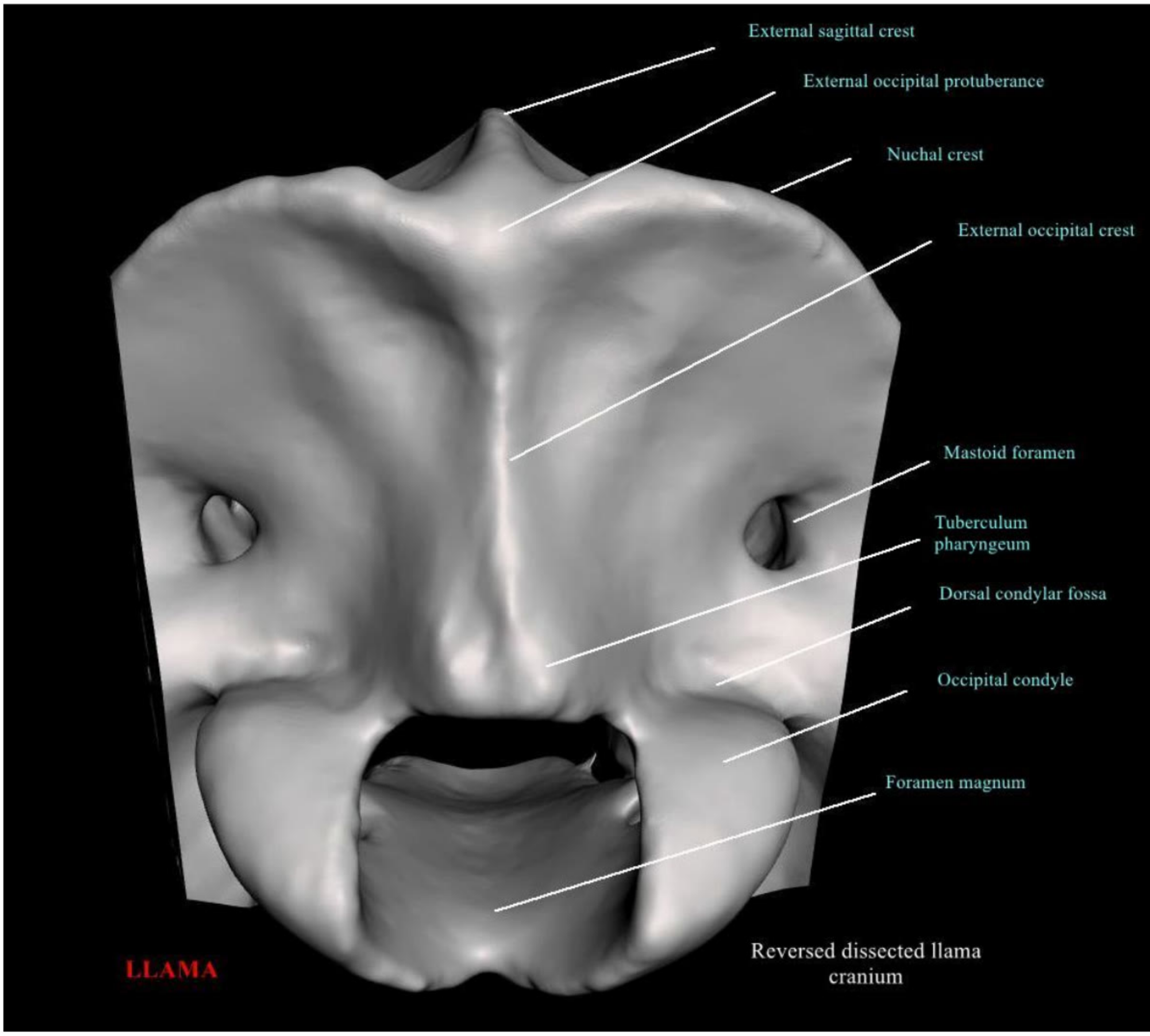

Figure 4: 3D CT model of the digitally dissected cranium of the llama skull viewed from the back showing anatomical details. It will be compared with the face of the tridactyls.

SECTION III: FINDINGS

- *López* had included only the skull of '***Josefina***' in his study and comparison. In this study, 3 tridactyl skulls have been included, namely from '***Josefina***', '***Luisa***' and '***Alberto***'. The facial features of these 3 individuals show some differences e.g. the supraorbital ridge is less conspicuous in '***Alberto***' . *(Figure 5)*
- The llama cranium alone is larger in size overall as compared with all 3 tridactyl complete skulls. The tridactyl skulls have slightly different shape, being more rounded at the top and less bulging at the side, whereas the llama cranium is rather flat at the top. *(Figures 6,7)*
- The llama cranium is composed of very thick bones (twice or more) with smooth inner and outer surfaces and rather robust bone structures such as nuchal crest and external sagittal crest. The tridactyl skulls all show thinner intact bones with prominent brain convolution markings on the inner skull surface. No counterpart for external sagittal crest is found in all tridactyls. The nuchal crest in llama cranium is much more robust as compared with the supraorbital ridges in the tridactyls. *(Figures 7,8,9,10)*
- The large orbits in tridactyls are prominent facial features with well defined rim and presence of an elongated slanting orbital fissure in each orbit. The llama cranium only features smooth plain bones harbouring a rounded mastoid foramen and completely lack the counterpart for the tridactyl orbits. *(Figure 10)*
- The foramen magnum and associated neck structure are located at the skull base in tridactyls. The foramen magnum originally situated at the back of the skull, being a big hole in the llama cranium had been transposed from back to front to correspond with the mouth parts of the tridactyls. The tridactyls have conical shape mouth with complex superior and inferior mouth plates hinges at the sides. *(Figures 10,11)*
- The prominent tuberculum pharyngeum located above the foramen magnum in llama cranium cannot be mapped onto the vestigial nose of the tridactyls. They are different in shape. *(Figures 6,10)*
- The tridactyls have multiple sinus spaces within the skull bones. These are lacking in llama cranium. *(Figure 17)*
- The occipital part of the tridactyl skull shows intact bone with occipital suture and presence of internal occipital crest. The corresponding part of the llama cranium belongs to the frontal and ethmoidal regions of the llama skull showing a large cut surface with irregular gaping bones with 2 large openings. *(Figures 6,7,8,12,13)*
- Foramina in skull base of llama cranium do not correspond to that found in tridactyls. *(Figures 14,15)*

SECTION III: FINDINGS (continued)

- Special peculiarities found in tridactyls are 3 discrete large and some smaller bony depressions in the facial bones. These are speculated to be heat pits. Such structures are unique and cannot be a feature in llama cranium. *(Figure 16)*
- The detailed shape of the otic capsules of llama and tridactyls including their internal structures do not match. *(Figures 17,18)*
- Digital endocasts created from 3D CT models of llama cranium and tridactyl skull showed multiple differences. *(Figures 19,20)* Direct volume measuring of the digital endocast of llama cranium shows 244 ml and is 14% larger than the volume of the skull of '***Luisa***' measuring 214 ml.
- Notable differences between llama cranium and tridactyl skull are listed in tabulated form. *(Figure 21)*

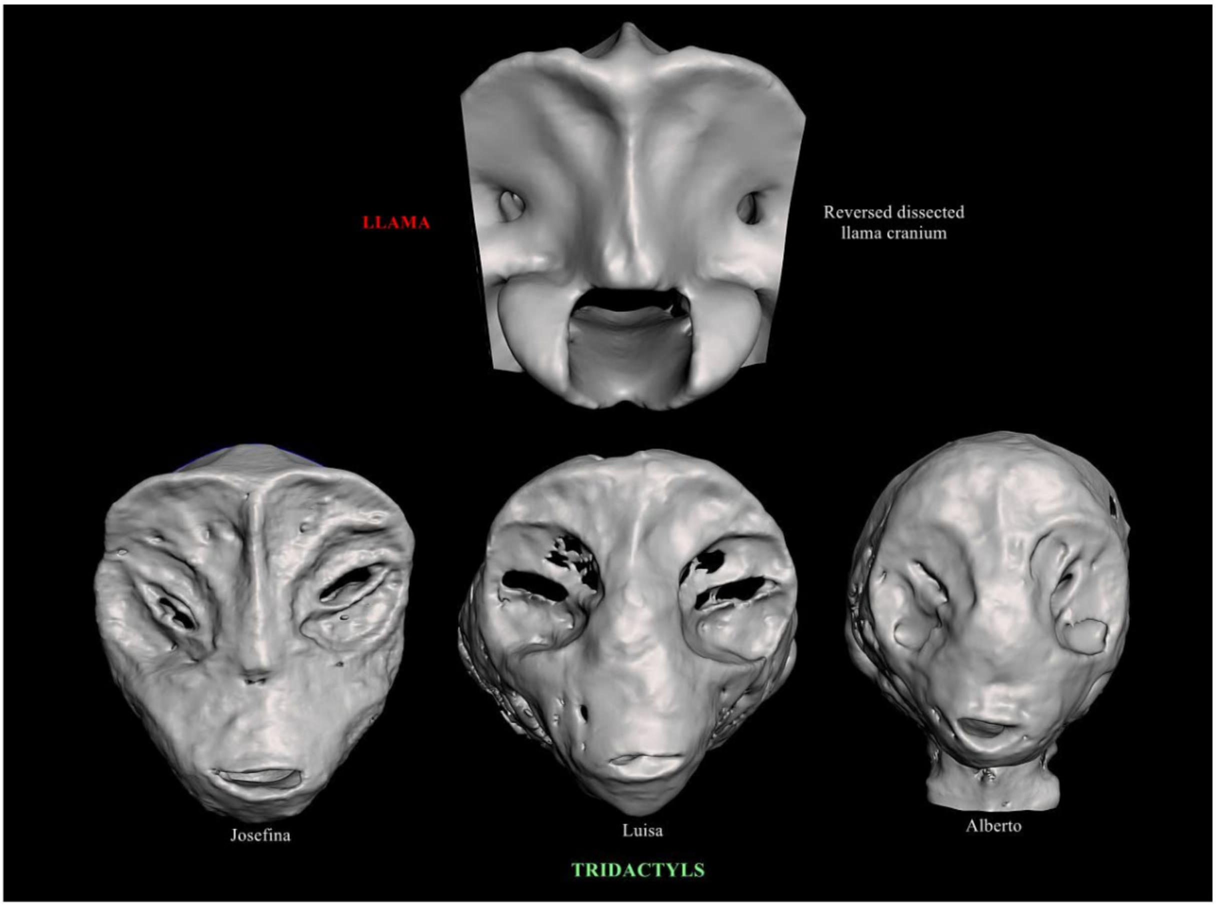

Figure 5: 3D CT model of the digitally dissected 'face' formed by the back of the llama cranium *(upper image)* comparing with faces of the 3 tridactyl skulls *(lower images)*. Grossly, the tridactyl skulls show a cordiform-shaped face with a pointed chin. Note the very large eye sockets with well-defined rims containing elongated slanting orbital fissures. There are significant individual variations in bony ridges delineating the top part of the face. In Alberto, the forehead region is almost rounded without distinct ridges.

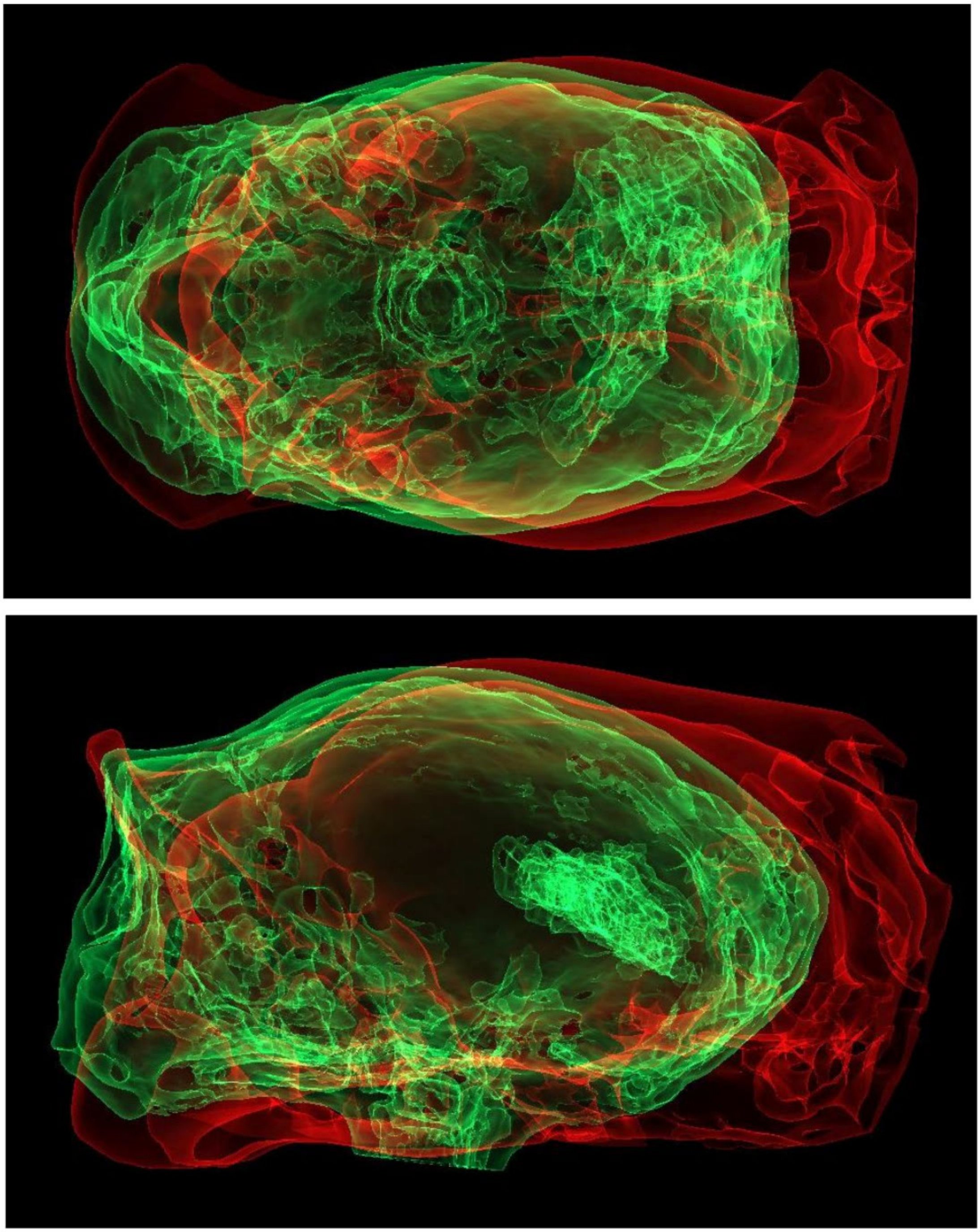

Figure 6: 3D CT model of llama cranium *(in red)* aligned against the antero-superior aspect with the skull of '***Josefina***' *(in green)* in overlapping fashion and viewed in semi-transparency. Top view *(upper image)* and left side view *(lower image)* showing larger size of the llama cranium with less rounded contour.

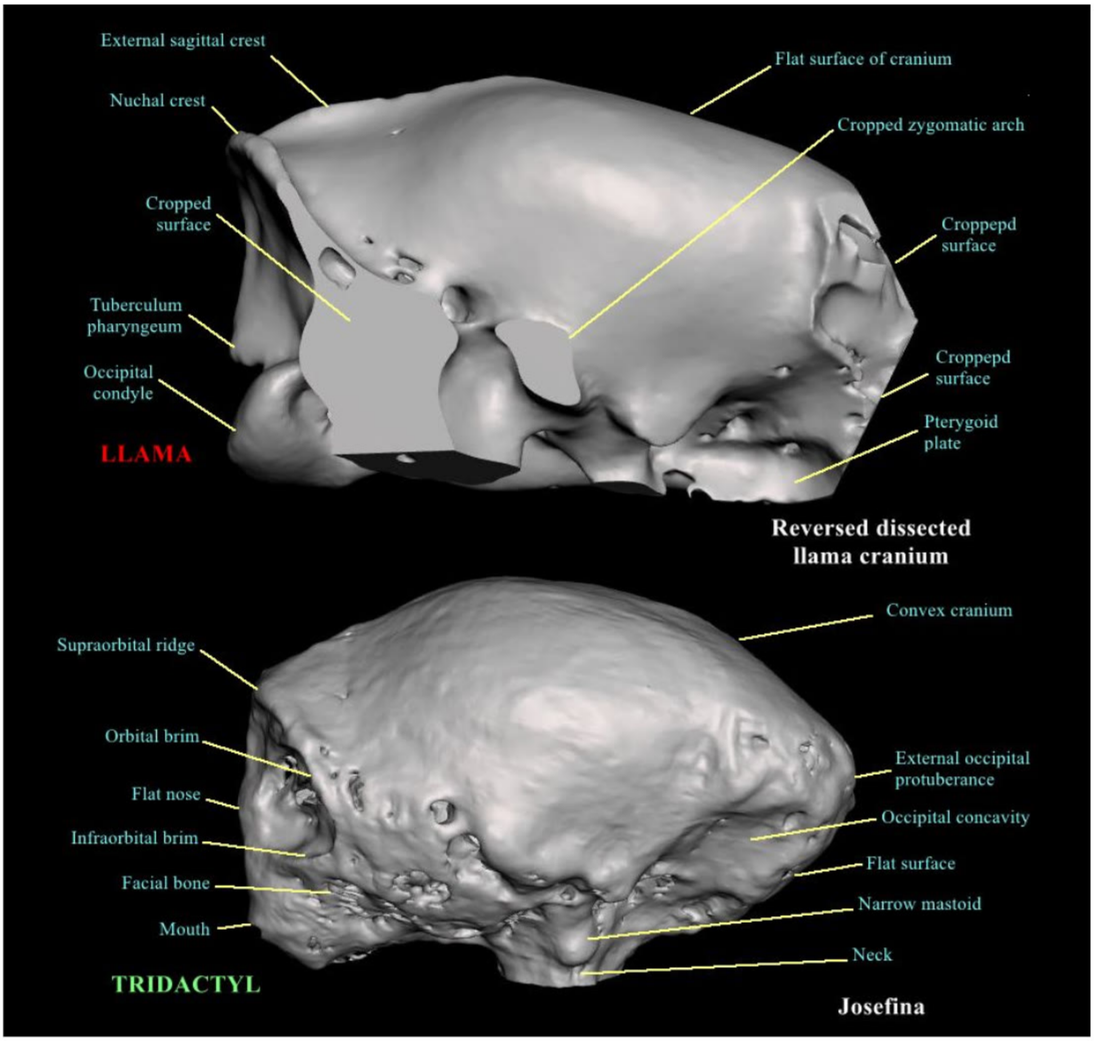

Figure 7: Comparison of lateral view of 3D CT models of llama cranium *(upper image)* and skull of '***Josefina***' *(lower image)*. Points of gross discrepancy are labelled. There are prominent cropped surfaces in the massive paracondylar process cum typmpanic bulla, zygomatic arch and in the foveae ethmoidale of llama cranium. The skull top shows a rather flat surface with presence of a prominent external sagittal crest in llama cranium. On the other hand, the tridactyl skull shows a more rounded contour at its top, more refined features in the mouth and facial bones inferiorly. The occipital region of tridactyl shows solid bone with a large smooth concavity on both sides. Narrow mastoid processes are found on either side of the neck. No evidence of deteriorated bone was noted in '***Josefina***'.

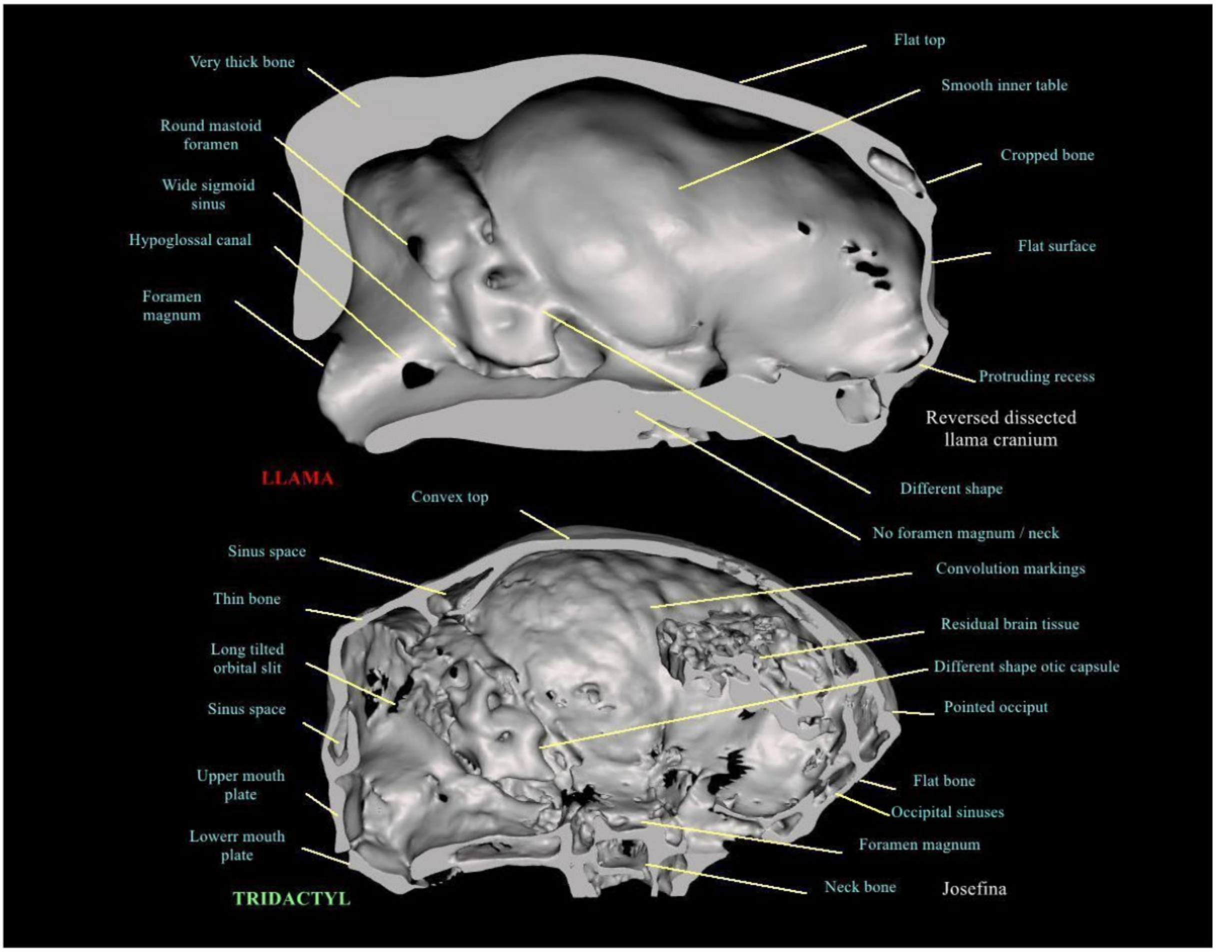

Figure 8: Comparison of inner aspect of right half of 3D CT models of llama cranium *(upper image)* and skull of '***Josefina***' *(lower image)*. Points of gross discrepancy are labelled. Note the very thick solid bones in llama cranium particularly at skull base and above foramen magnum. The inner skull table is smooth. In contrast, the tridactyl skull shows well defined but thin bones. Structured upper and lower mouth plates are present contrasting with the hole formed by the foramen magnum in llama. Behind the mouth apparatus, there is absence of any hole that could match with the hypoglossal canal of the llama cranium. The foramen magnum of the tridactyl is located in the mid segment of skull base with associated neck structure. No corresponding structures are noted in skull base of llama cranium.

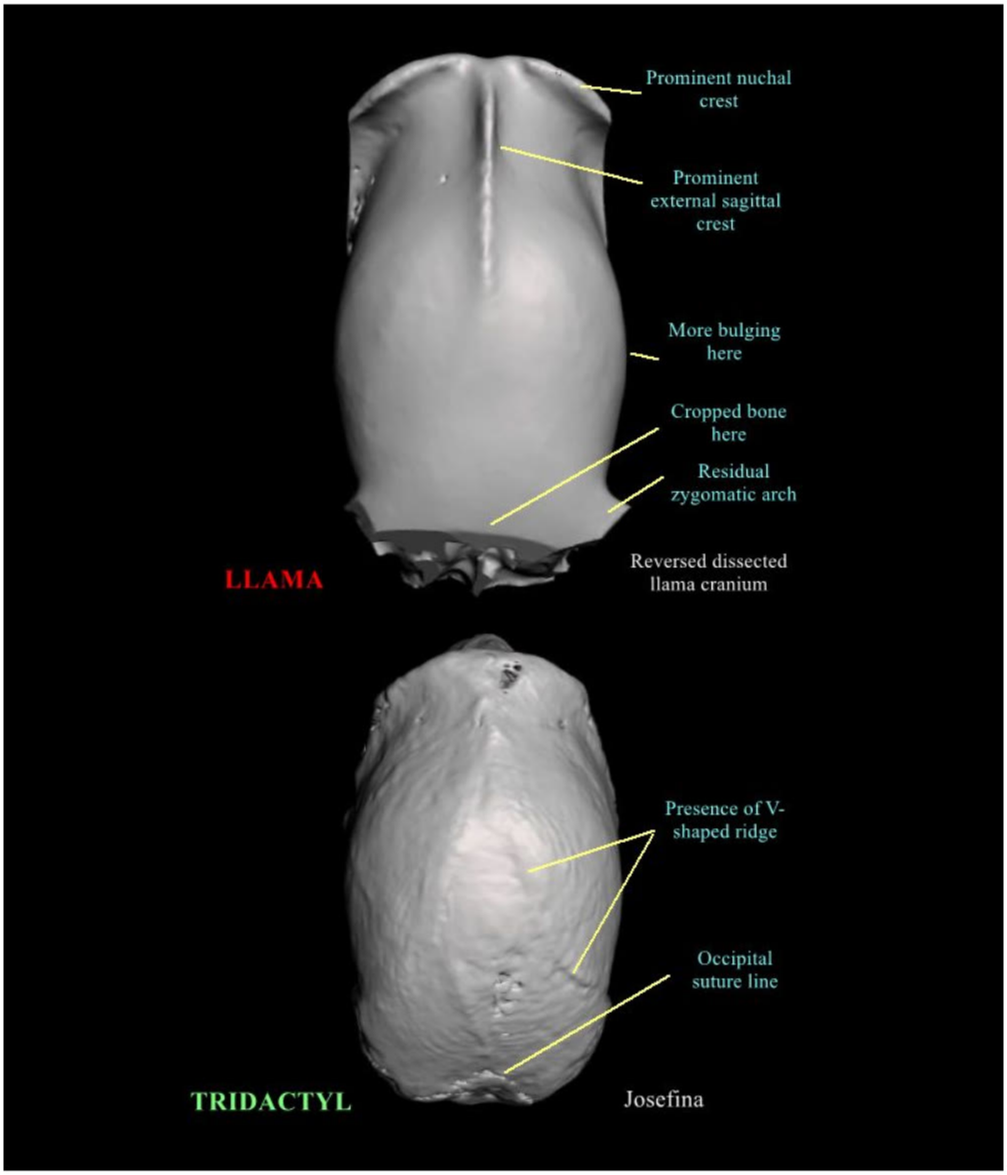

Figure 9: Comparison of top views of 3D CT models of llama cranium *(upper image)* and skull of '***Josefina***' *(lower image)*. Points of gross discrepancies are labelled. Note the larger size of the llama cranium with more localised lateral bulging. Prominent midline external sagittal crest is a feature in llama cranium not found on tridactyl. Instead, a faint V-shaped ridge can be seen on top of the tridactyl skull. The nuchal crest in llama cranium is much more pronounced as compared with the supra-orbital ridge of '***Josefina***'. Posteriorly, intact occipital bone and occipital suture are present in tridactyl contrasting with irregular bones with cropped surfaces in llama cranium.

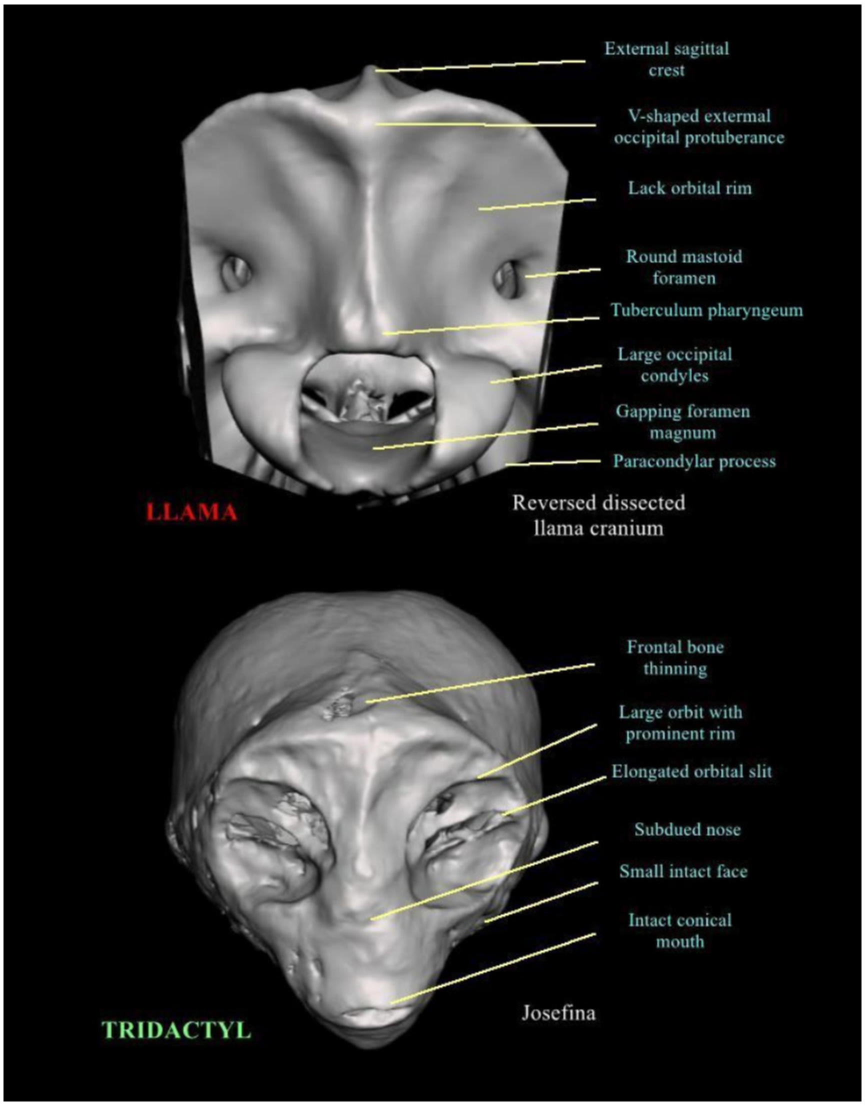

Figure 10: Comparison of 3D CT models of llama cranium *(upper image)* with facial feature in skull of '***Josefina***' *(lower image)*. Points of gross discrepancies are labelled. Note in particular the gross differences in the orbits. Whereas in '***Josefina***', the orbits show clearly defined rim, thin bone and long slanting orbital fissures, in llama cranium only a rounded mastoid foramen is present, hardly matching the tridactyl orbits. External sagittal crest, a constant feature in llama skull is not found in the tridactyls. Furthermore the conical mouth with articulated upper and lower mouth plates in tridactyls cannot be accounted for in the large opening of the llama foramen magnum. The massive bones in paracondylar processes, tympanic bullae and large occipital condyles in llama cranium contrast with the delicate structured thin bones in the face of tridactyl.

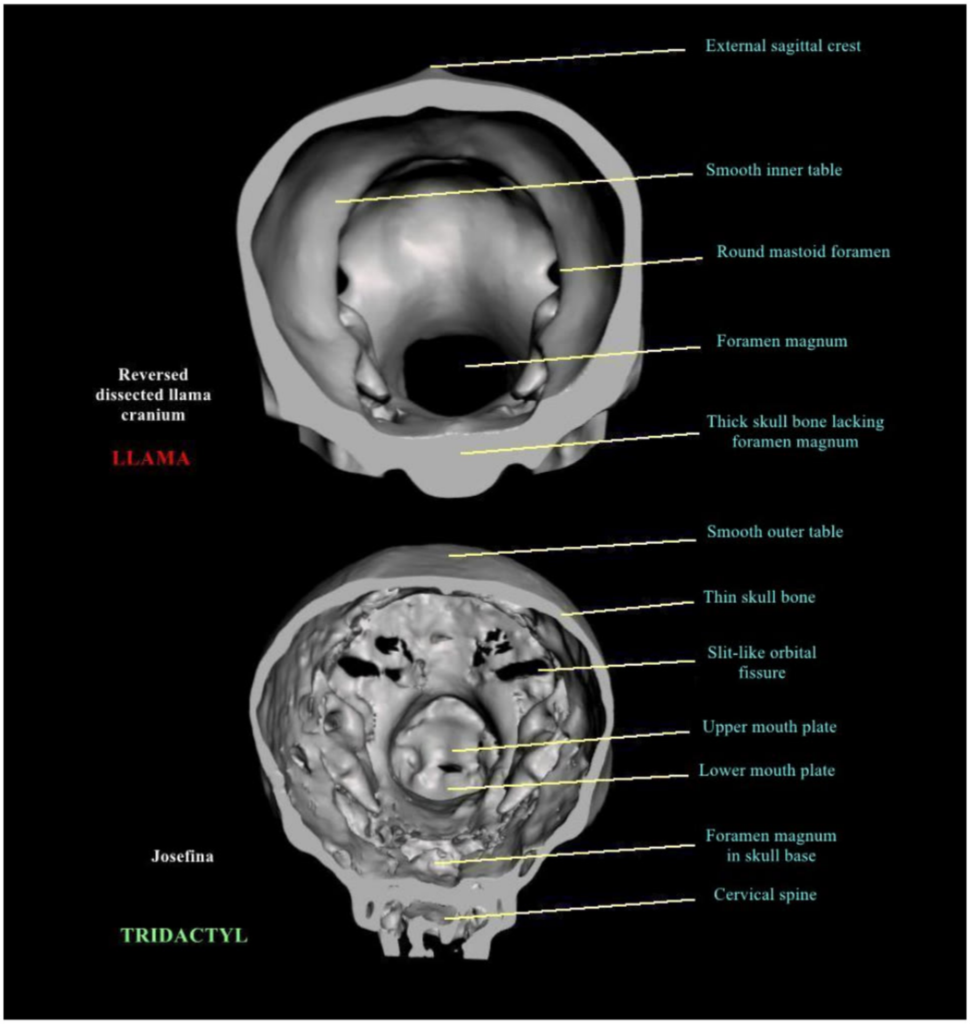

Figure 11: Comparison of front sections of 3D CT models of llama cranium *(upper image)* against the skull of '***Josefina***' *(lower image)* viewed from inside. Points of gross discrepancies are labelled. Note the smooth internal surface of llama cranium and the big hole formed by the foramen magnum. Articulated upper and lower mouth plates are found in '***Josefina***' in this location. The round mastoid foramen placed more laterally in llama cranium would correspond to the slanting slit-like orbital fissures in tridactyl. Foramen magnum is found at the skull base of '***Josefina***' but thick solid bone is noted in llama cranium in the same locality.

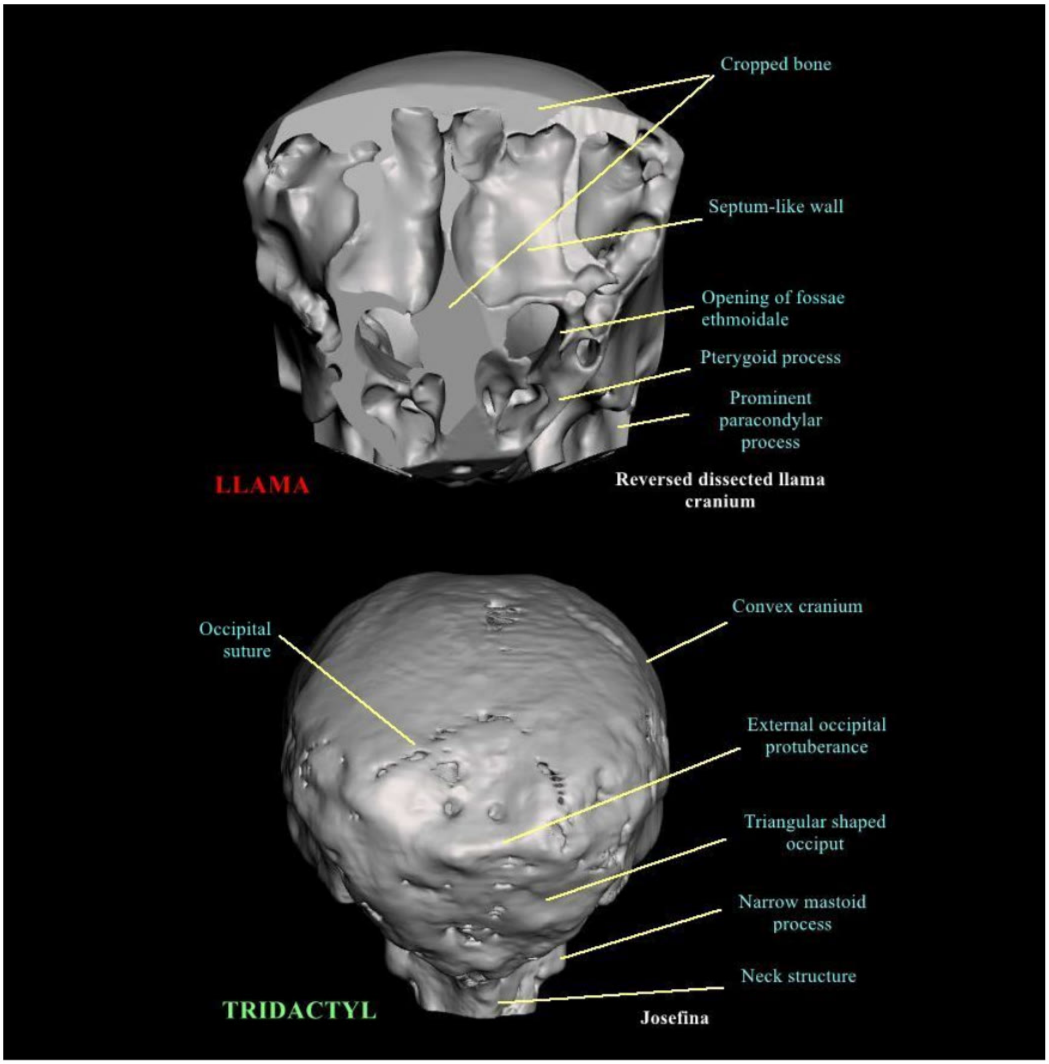

Figure 12: Comparison of back section of 3D CT models of llama cranium *(upper image)* and skull of '***Josefina***' *(lower image)*. Points of gross discrepancies are labelled. The tridactyl skull has intact bones forming external occipital protuberance with a flat triangular surface below. The occipital suture is visible. The corresponding part of the llama cranium is a cropped surface across the frontal bone and 2 openings in the fossae ethmoidale with irregular bone edges.

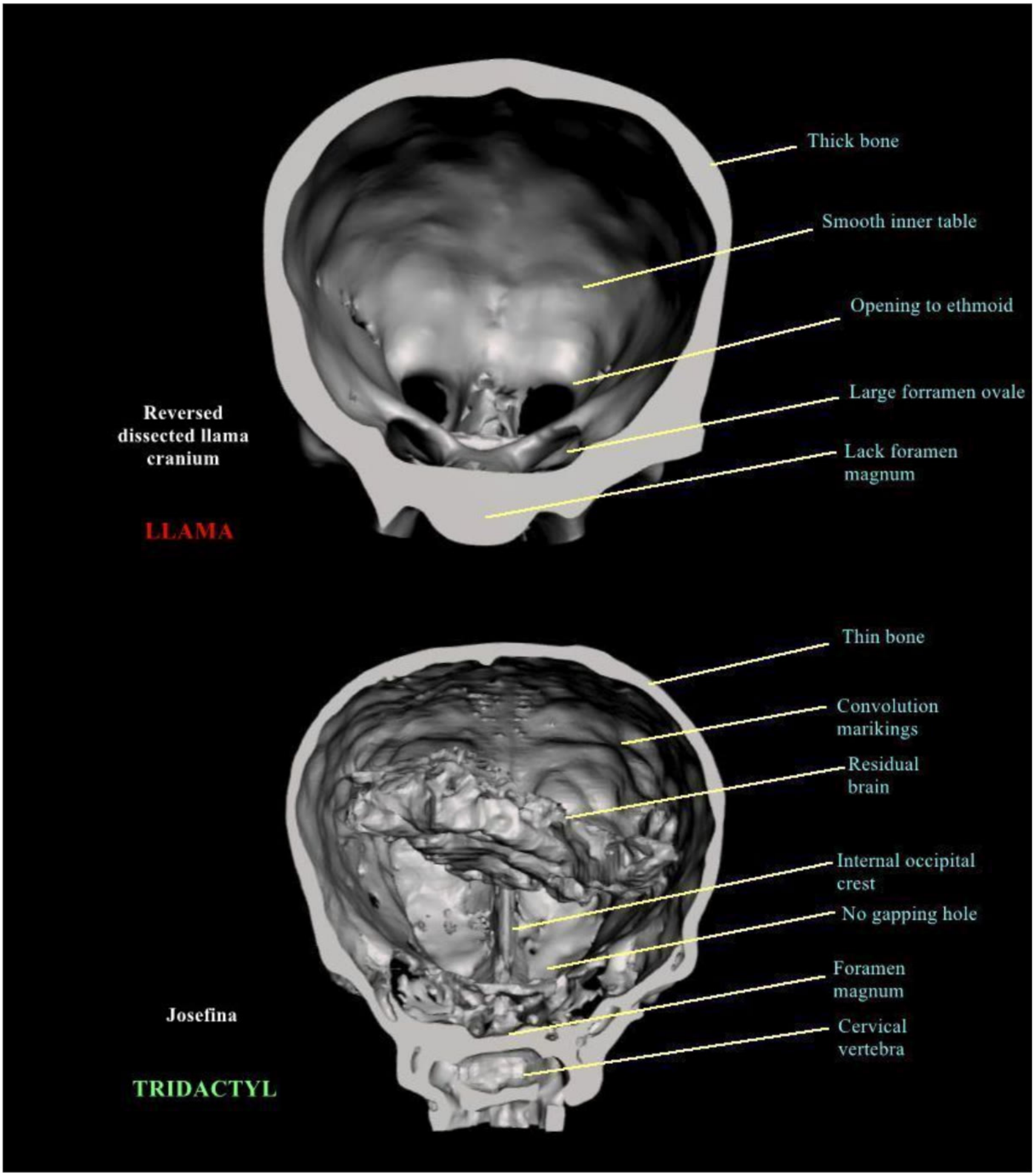

Figure 13: Comparison of back section of 3D CT models of llama cranium *(upper image)* and skull of '***Josefina***' *(lower image)* viewed from the inside. Points of gross discrepancies are labelled. The tridactyl skull has a more pear-shaped cross-section with thin bones. It shows prominent brain convolution markings on its inner surface whereas such surface is smooth in llama cranium. Residual brain tissue is noted within the skulls of '***Josefina***' and '***Alberto***'. There is a midline internal occipital crest in tridactyl skull that is absent in llama cranium. The posterior wall in tridactyl skull is intact whereas in llama cranium, 2 large openings communicating with fossae ethmoidale are present.

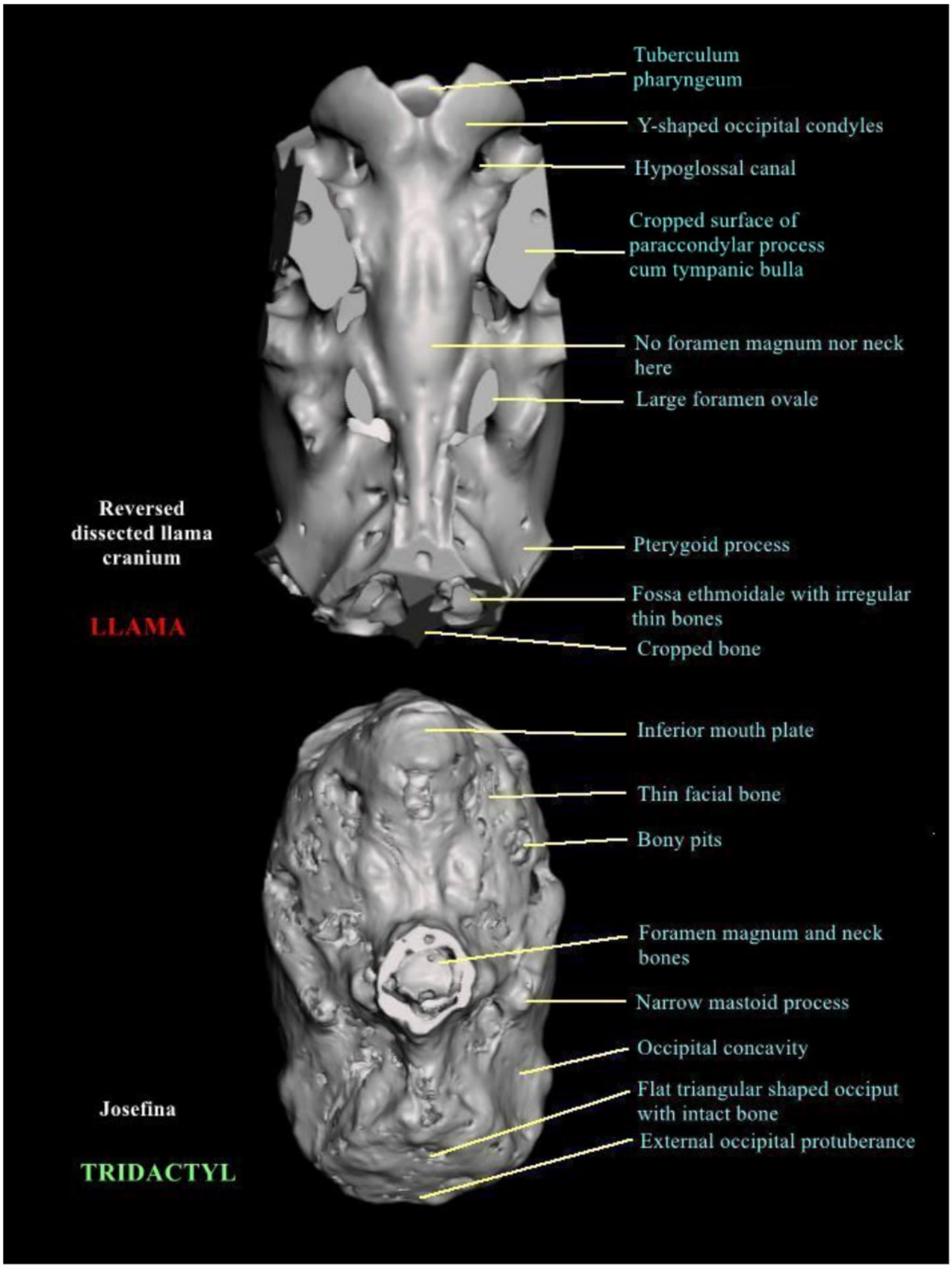

Figure 14: Comparison of basal views of 3D CT models of llama cranium *(upper image)* and skull of '***Josefina***' *(lower image)*. Points of gross discrepancies are labelled. Note the Y-shape configuration formed by the occipital condyles cum tympanic bullae anteriorly and the pterygoid processes posteriorly in llama cranium. Such features are not present in tridactyl skull. The foramen magnum occupies the mid portion of the tridactyl skull base bordered by a thin mastoid processes on either sides, not a feature in llama cranium.

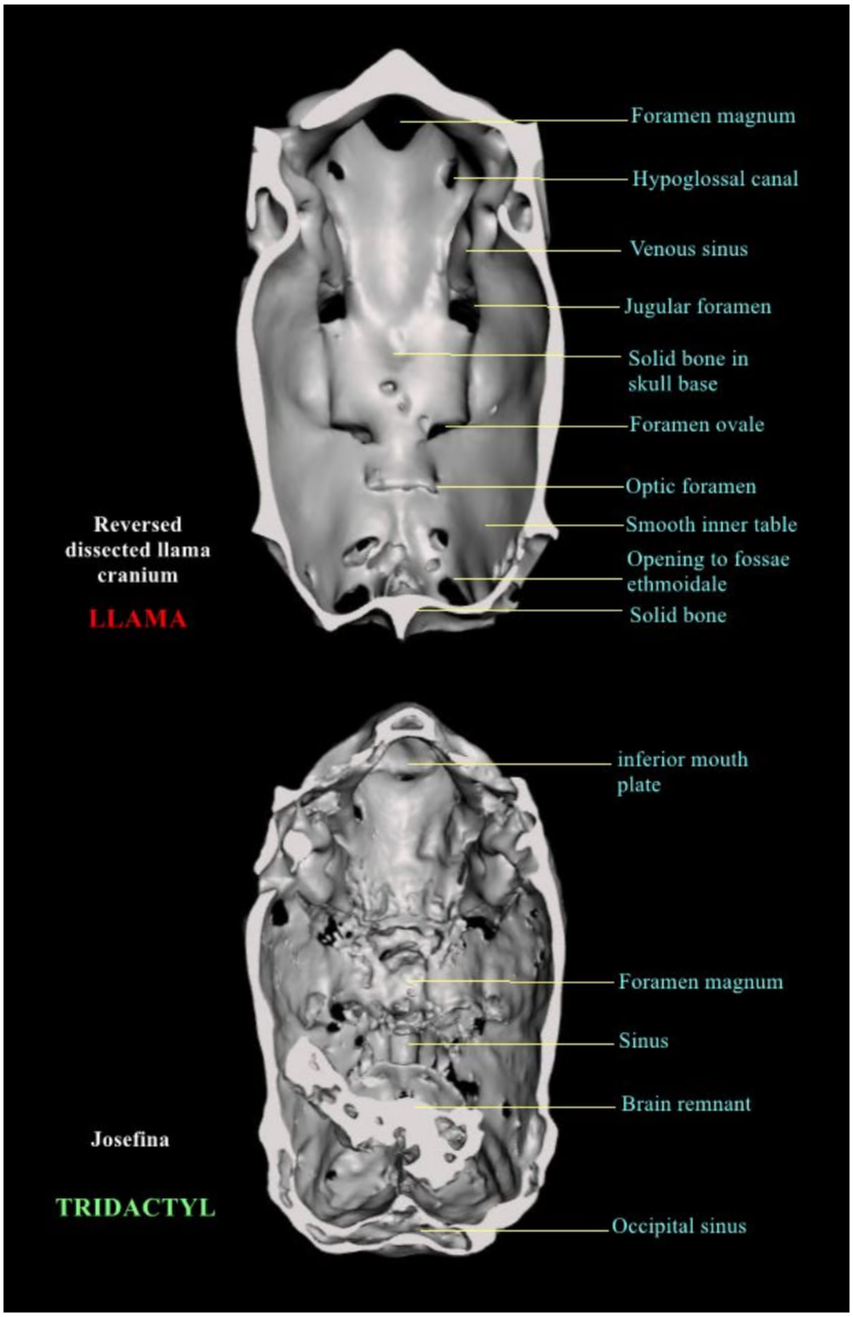

Figure 15: Comparison of lower cut sections of 3D CT models of llama cranium *(upper image)* and skull of '***Josefina***' *(lower image)*. Points of gross discrepancies are labelled. Note the foramen magnum occupies the mid portion of the tridactyl skull base that is not a feature in llama cranium.

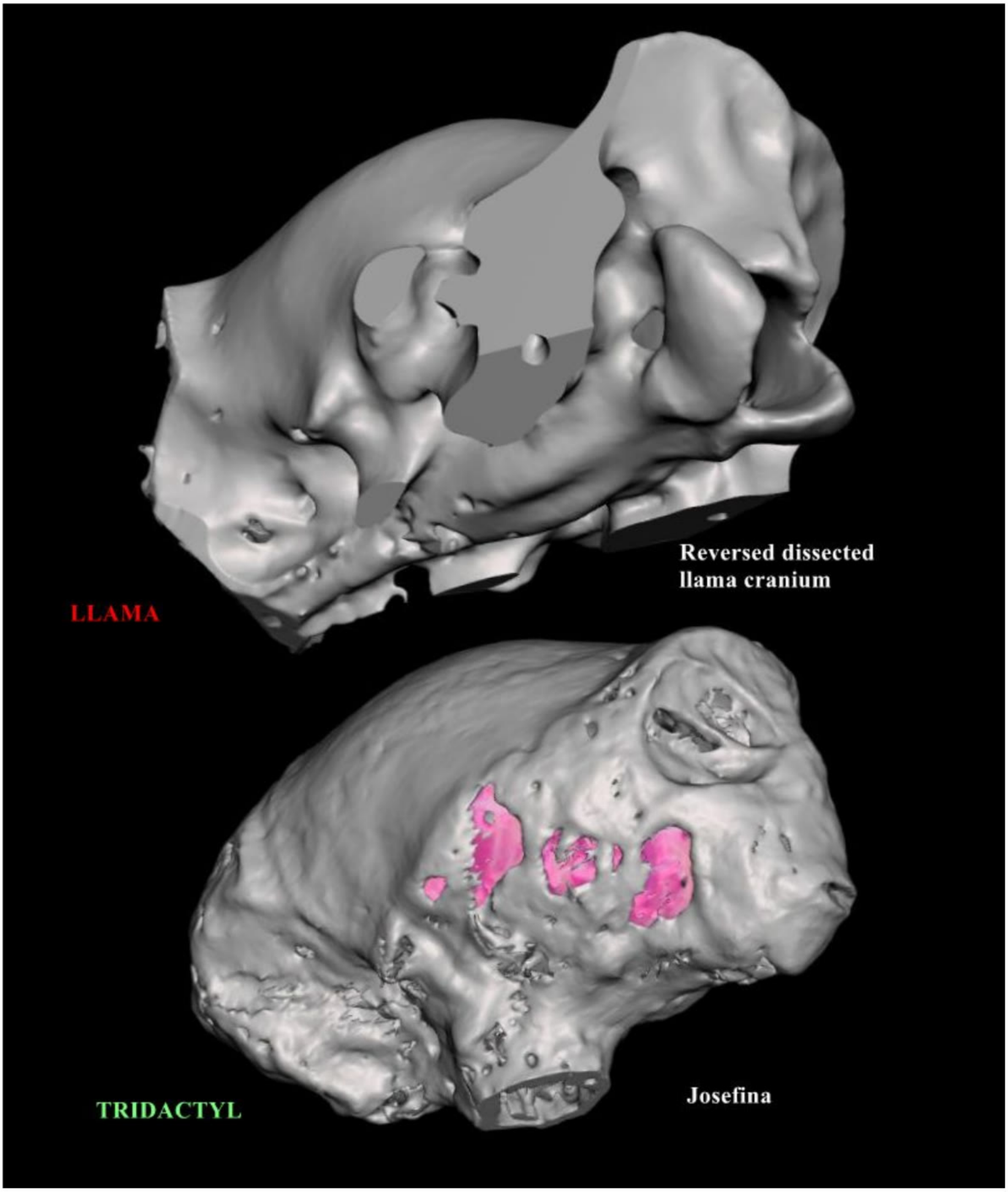

Figure 16: Comparison of 3D CT models of llama cranium *(upper image)* with facial features in skull of '***Josefina***' *(lower image)*. Note the presence of 3 large bony depressions *(in pink)* suspected to be heat pits in tridactyl face. The middle one is related to the otic capsule internally. Note the well defined margins and slanting slit in tridactyl orbit. Such structures are not a feature in llama cranium.

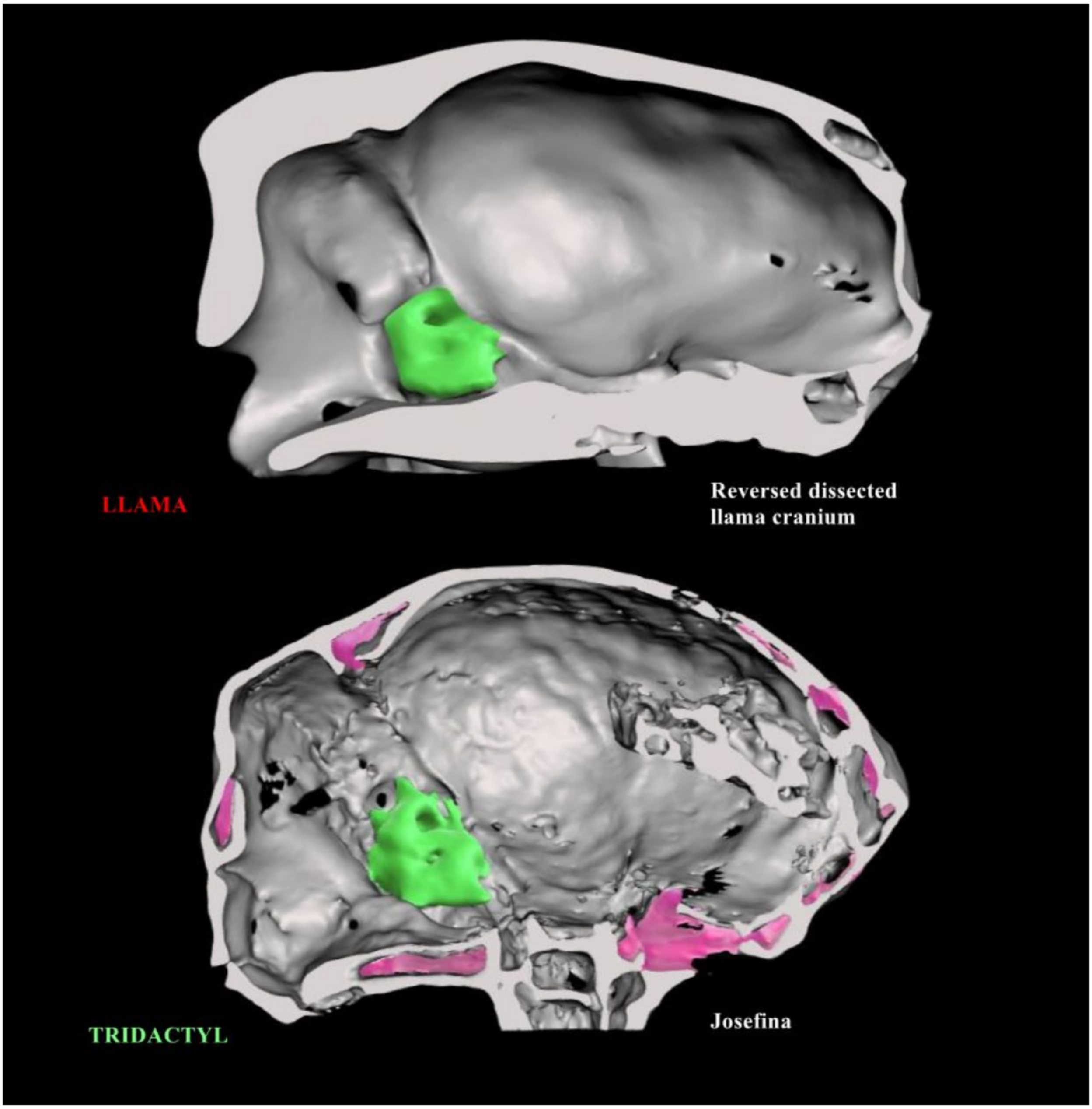

Figure 17: Comparison of lateral views of right section of 3D CT models of llama cranium *(upper)* and skull of '***Josefina***' *(lower)*. Note the thin skull bone in tridactyl containing multiple sinus spaces *(in pink)* whereas the bone in llama cranium is much thicker and more solid. The otic capsules are isolated by segmentation for comparison *(in green)*.

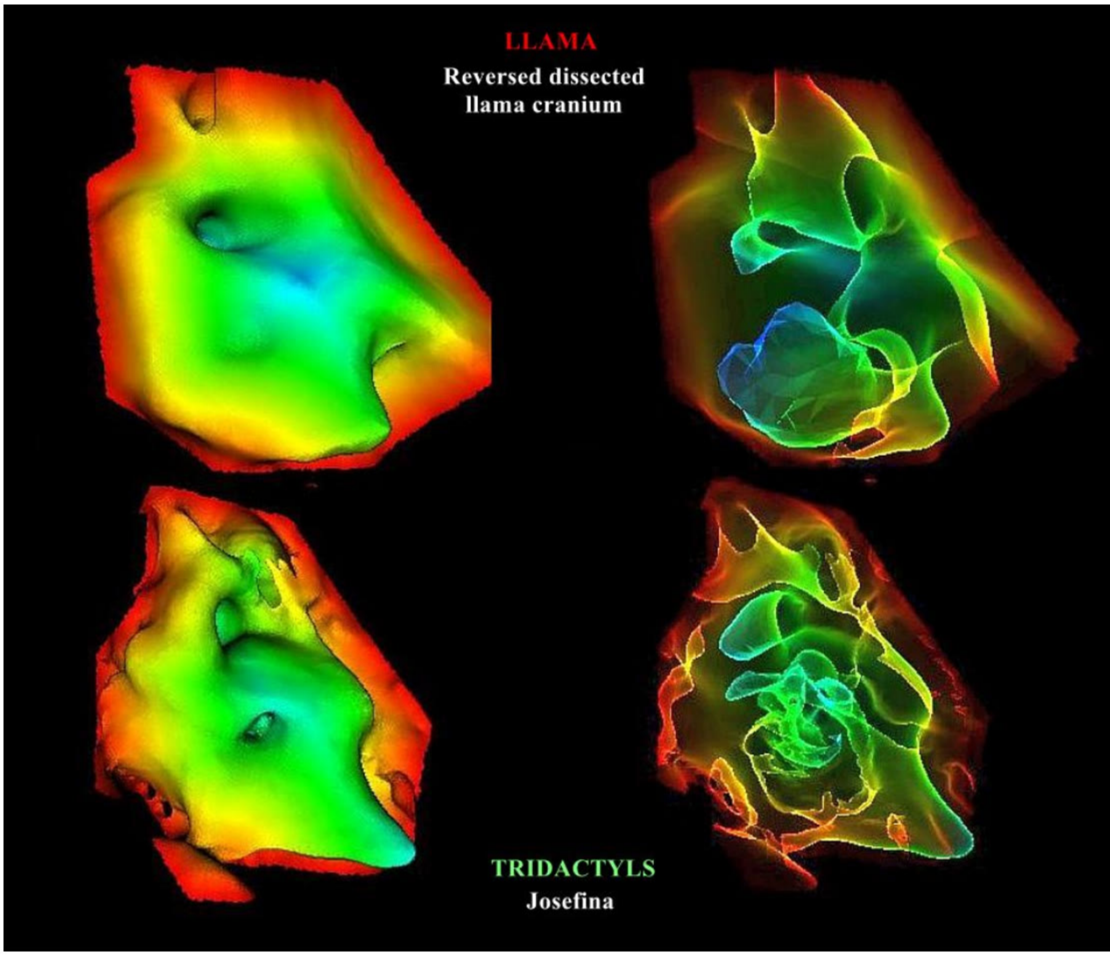

Figure 18: Comparison of cropped sections of 3D CT models of right otic capsules in llama cranium *(upper row)* against that of '***Josefina***' *(lower row)*. The surface view *(left)* and semi-transparent view *(right)* show structural differences.

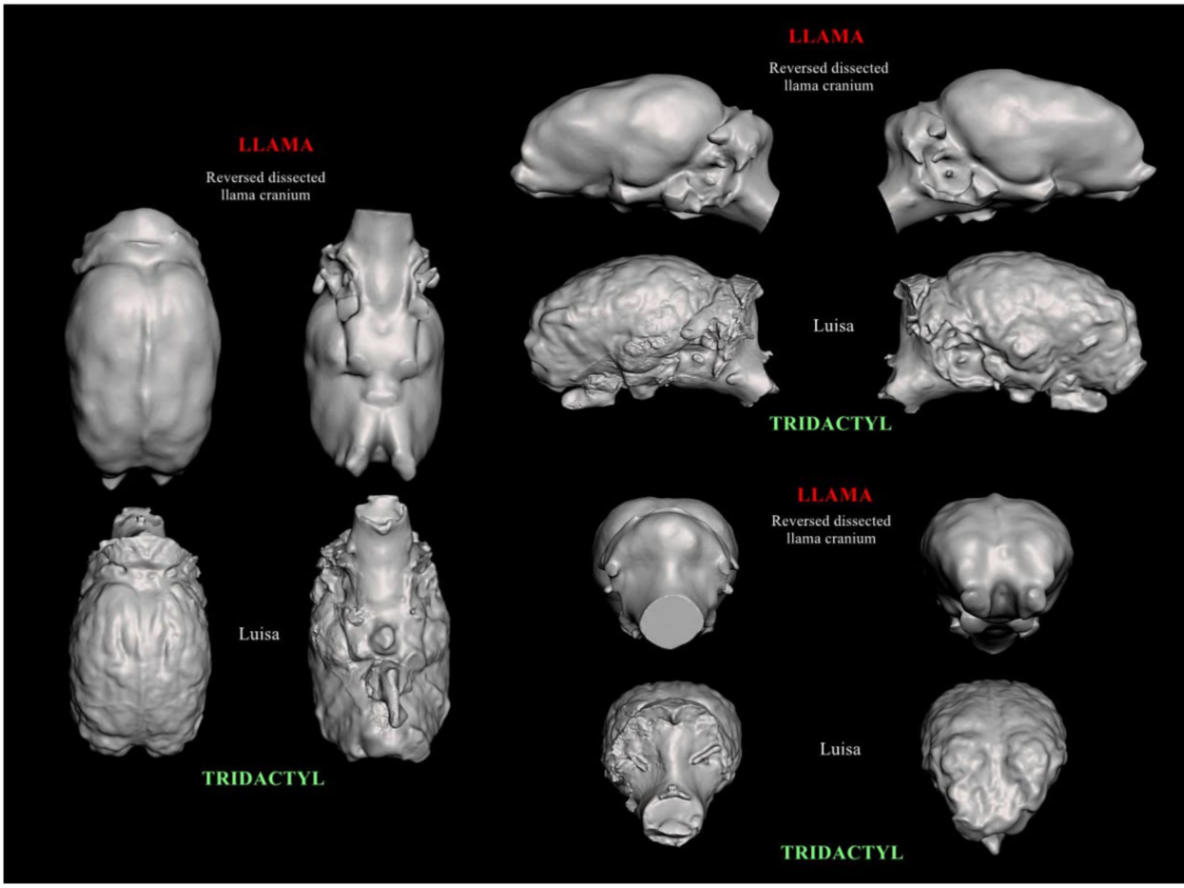

Figure 19: Comparison of digital endocasts created from 3D CT models of llama cranium *(L)* and skull of tridactyl '***Luisa***' *(T)* shown in various projections. *(Note: No brain remnant is found in skull of '**Luisa**' and is useful instead of '**Josefina**' for creation of digital skull endocast)*.

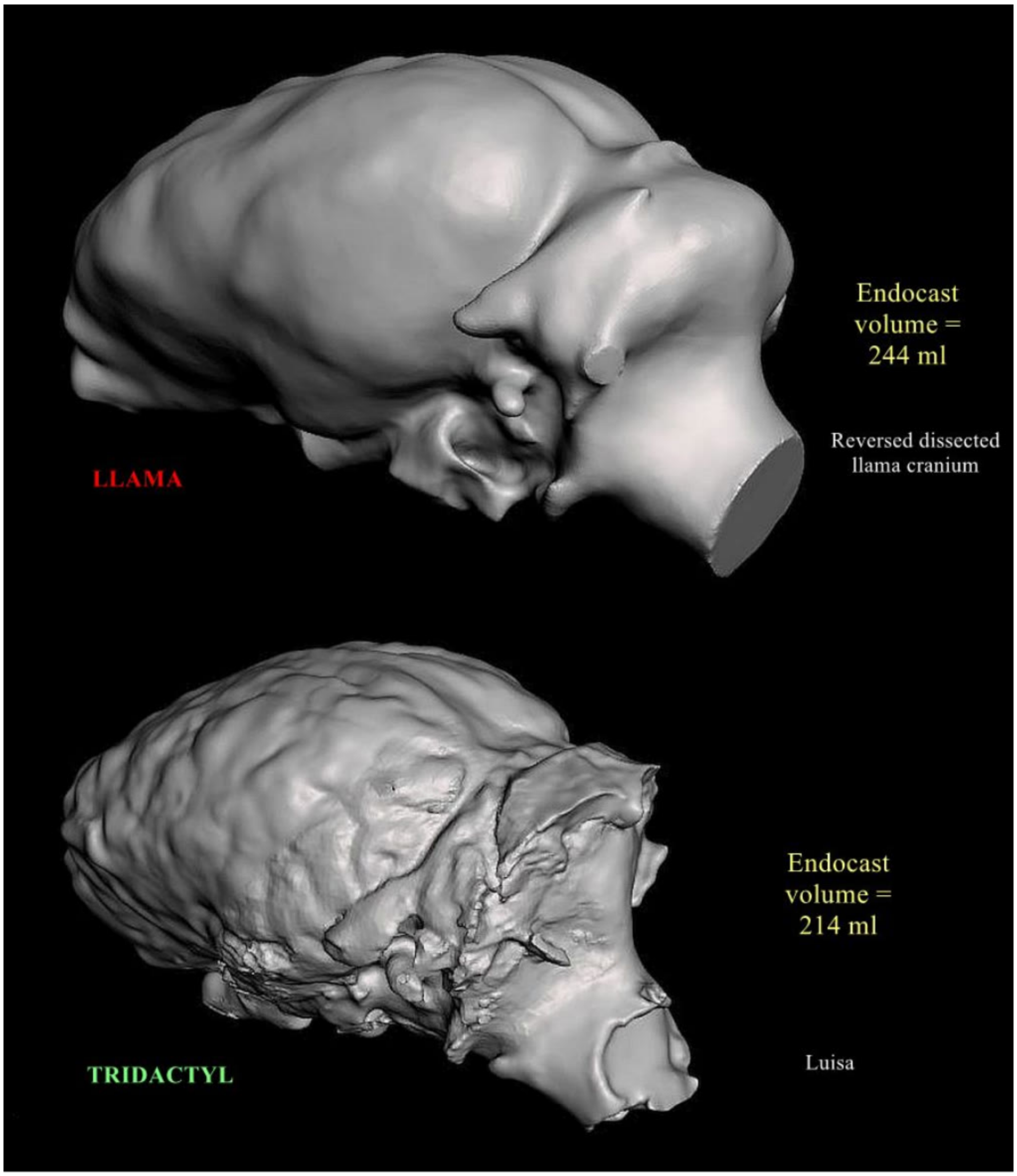

Figure 20: Comparison of digital endocasts created from 3D CT models of llama cranium and skull of tridactyl '***Luisa***'. The capacity in llama cranium is about 14% larger as compared with the skull of '***Luisa***'.

	COMPARE	REVERSED DISSECTED LLAMA CRANIUM	TRIDACTYL SKULL
1	***Size***	Larger	Smaller
2	***Bone thickness***	Thick (more than twice)	Thin
3	***Endocast volume***	244 ml (12% larger)	214 ml
4	***Skull vault***	Solid	Numerous sinuses
5	***Inner surface of skull***	Smooth	Prominent convolution markings
6	***Contour of upper surface of skull***	Smooth and flat	More rounded
7	***Contour of occiput***	Irregular cropped bones in ethmoid with 2 openings	Well formed occiput, triangular in shape with intact bone
8	***Internal occipital crest***	None	Present
9	***Crop marks***	Multiple, prominent	None
10	***Foramen magnum location***	Front	Inferior
11	***Paired occipital condyles***	Prominent	None
12	***External sagittal crest***	Prominent	Absent
13	***Mouth plates***	None	Upper and lower mouth plates
14	***Hypoglossal canals***	Behind foramen magnum	None
15	***Nasal bones***	Tuberculum pharyngeum	Flat nose
16	***Paracondylar process***	Prominent	None
17	***Tympanic bulla***	Prominent	None
18	***Heat pits in facial bones***	None	3 large bony depressions
19	***Eye slits***	Round mastoid foramen	Elongated slanting orbital fissures
20	***Orbital brim***	Absent	Prominent
21	***Supraorbital ridge***	Prominent nuchal crest	Variable in different specimens
22	***Otic capsule***	Different shape	Different shape
23	***Mastoid process***	Solid and large	Narrow, contain air spaces
24	***Neck bones***	None	Yes
25	***Other body parts***	Not available	Whole body

Figure 21: Table comparing notable differences between llama cranium and tridactyl skull.

SECTION IV: DISCUSSIONS

This detailed comparative scientific study based on CT-generated 3D models suggests that a reversed dissected llama cranium compared with the skulls of tridactyls shows very significant differences and could not be the same.

In *López* peer review paper, he concluded that '***Josefina***' head is *(quote)* "*composed of a llama deteriorated braincase"*. He placed strong and repeated emphasis on the word '*deteriorated*' in order to explain all his findings and to cover up all imaging discrepancies. However on review of his findings, it was found that he was comparing models created using different methodologies. Our analysis suggested that the llama skull model downloaded from DigiMorph was created using **shaded-surface-display (SSD)** for 3D model creation with single threshold set specifically for bone density. Our analysis also suggested that the 3D model for '***Josefina***' that *López* had used in his illustrations was created using **direct volume rendering (DVR)**. DVR is based on ray tracing technique by summation of different densities along a path and projecting the resulting composite value onto an assigned colour scale. In order words, in DVR, **soft tissue densities can be admixed with bone densities** to create the final image depending on the setting. The scale can be bias towards a wider or narrower range of densities or the CT density value by adjusting the window width and window level similar to the use of dynamic range in photos. This could have lead to misinterpretation by *López* of a '*deteriorated braincase*' in '***Josefina***' when he had used an inappropriate window setting for interpretation of the CT dataset, particularly when '***Josefina***' has thin skull bone with prominent brain convolution markings and there are numerous sinus spaces within the skull bone.

In this study, a like-for-like comparison with enough detail was made using SSD in both cases. This study showed no evidence of deteriorated braincase. The difference in bone thickness was genuine. Therefore *López* paper was in fact 'an argument based on a false premise'.

The findings that *López* made were confusing and important issues were being neglected. For example, he described in great detail the complicated anatomy in the mouth part of '***Josefina***' but failed to describe how the llama skull could have imitate this degree of complexity by incorporating foreign bones.

His findings were also conflicting and unexplained. In page 50 of his paper, he stated *(quote)* "*There are features that do not correspond....*" relating to presence of *(quote)* "*external sagittal crest in llama skull that is not present in Josephina's skull.*" etc. Again he found it hard to explain how the llama cranium can mimic the occipital area of '***Josefina***', *(quote)* "*The occipital area is the most puzzling one, as there are many opening with areas of solid bone.*"

SECTION IV: DISCUSSIONS (continued)

López had included evidences based only on the skull of tridactyl '***Josefina***' without addressing the context of the whole skeleton e.g. how does the llama cranium relate to the rest of the skeleton, how to relate to skin and soft tissue, and to explain how to insert the cranium inside the specimen despite intact skin covering.

In *figure 17 on page 63* of his paper, he attempted to cover part of the cervical region illustrating a cord behind the cervical spine. He claimed *(quote)* "*they may be actual veins or, for fixing purposes, vegetable strings or intestines.*". As a scientific research paper, he did not provide any scientific evidence to substantiate his claim and he had not ruled out the possibility of the structure being the cervical spinal cord. This claim is deceptive, unscientific and imaginative.

There are multiple specimens of tridactyl skulls sharing some individual variations. Only a single llama skull is studied. It is illogical for him to generalised or justify a claim against the whole group of J-type tridactyls.

SECTION V: CONCLUSION

Base on this detailed comparative study using CT generated 3D models, the final verdict is:

'TRIDACTYL SKULL IS NATURAL AND IS DIFFERENT FROM LLAMA SKULL'

SECTION VI: REFERENCES

1. *José de la Cruz Ríos López* et al. (2021) **Applying CT-scanning for the identification of a skull of an unknown archaeological find in Peru** International Journal of Biology and Biomedicine Volume 6, 46-65 ISSN: 2367-9085
2. **Digital Morphology**: A National Science Foundation Digital Library at The University of Texas at Austin (DigiMorph) (https://www.digimorph.org)
3. **Tridactyls.org** (https://tridactyls.org)
4. Software: Osirix (https://www.osirix-viewer.com)
5. Software: Meshmixer (https://meshmixer.org)
6. *Petronela Mihaela ROSU* et al. (2024) **Morphological particularities of the *Lama glama* skull** Scientific Works. Series C. Veterinary Medicine, LXX(2) 24-29. ISSN 2065-1295

SECTION VII: DISCLAIMER

- The author is a voluntary independent researcher.
- The views and opinions expressed in this articles are those of the author and do not necessarily reflect the official view of Tridactyls.org.
- The information provided in this paper is for research and educational purposes only.
- No research grant/funding nor financial interests have been involved.

ABOUT DR. FUNG

Dr. K H Fung is a retired radiologist with over 40 years of experience in diagnostic radiology. His special interests include 3D medical visualization, interventional radiology and neuro-intervention.

Dr. Fung is also an artist in the domain of intersection of art and science utilising his expertise in 3D medical visualization. Dr. Fung was the first place co-winner in the '2007 International Science & Engineering Visualization Challenge' organized by Science magazine and National Science Foundation (USA).

His artworks had been exhibited in museums in various countries including USA, Europe, China, Australia and Hong Kong.

He had current exhibits in 2025 in the Hong Kong Museum of Medical Sciences (featuring stereoscopic 3D and 4D medical imaging and art) and in Nina Park (featuring the Nina wood fossils collection) in Hong Kong.

Through his collaboration with Science Photo Library, his interdisciplinary artworks bridging art and science had been made available to various international renowned digital media, magazines, books, and journals.